Journal of Arid Environments 237 (2026) 105708

Contents lists available at ScienceDirect

Journal of Arid Environments

journal homepage: www.elsevier.com/locate/jaridenv

Multi-decadal drought variability and regime dynamics in Darfur, Sudan (1981–2025)

Abdalrahman Ahmed [a,b,*], Kornel Czimber [a]

[a] Institute of Geomatics and Civil Engineering, Faculty of Forestry, University of Sopron, Sopron, Hungary Bajcsy-Zs 4, Sopron, 9400, Hungary
[b] Department of Forest and Environment, Faculty of Forest Sciences and Technology, University of Gezira, P.O. Box 20, Wad Madani, Sudan

ARTICLE INFO

Keywords:
Drought
SPEI
BFAST
Sahel
Sudan
Climate variability

ABSTRACT

Understanding drought dynamics in arid and semi-arid regions is essential for climate adaptation and sustainable resource management. This study assessed multi-decadal drought variability in Darfur, western Sudan, from 1981 to 2025 using the Standardized Precipitation–Evapotranspiration Index at a 12-month timescale (SPEI-12). Monthly precipitation and temperature records from North, West, and South Darfur were analysed using piecewise linear regression, Bayesian Information Criterion (BIC)-based breakpoint detection, and Breaks for Additive Seasonal and Trend (BFAST) analysis. A precipitation–temperature proxy was used for climatic water balance because potential evapotranspiration data were unavailable. Results revealed statistically significant positive SPEI-12 trends across all regions, indicating a gradual reduction in cumulative drought severity. West Darfur exhibited the strongest trend (0.0463 yr^{-1}; R^2 = 0.356), followed by South Darfur (0.0407 yr^{-1}; R^2 = 0.277), whereas North Darfur showed a weaker trend (0.0198 yr^{-1}; R^2 = 0.065) and greater interannual variability. Although piecewise regression detected no long-term structural breaks, BFAST identified episodic climatic transitions. Severe drought events persisted, particularly during the early 1980s and in recent years. Overall, drought evolution in Darfur is consistent with the broader post-1990s Sahelian hydroclimatic recovery while exhibiting pronounced spatial heterogeneity, providing a basis for drought monitoring and climate adaptation in arid environments.

1. Introduction

Drought is a complex hydroclimatic phenomenon characterized by prolonged deficits in water availability resulting from anomalies in precipitation and atmospheric conditions, including increased temperature and evaporative demand (Dai, 2011; Mishra and Singh, 2010). Unlike sudden-onset hazards, droughts develop gradually, vary across spatial and temporal scales, and are often difficult to define in terms of their precise onset and termination (Liu et al., 2023; Sreeparvathy et al., 2025). Its cumulative nature complicates impact assessment, particularly in arid and semi-arid environments where even small climatic deviations can produce substantial ecological and socio-economic consequences (Asfaw et al., 2021; Tirivarombo et al., 2018).

Globally, droughts are among the most economically damaging natural hazards, affecting agriculture, water resources, energy production, and ecosystem services (Alahacoon and Edirisinghe, 2022; Keshavarz and Karami, 2018). In dryland regions, recurrent drought constrains primary productivity, reduces rangeland carrying capacity, and intensifies land degradation processes (Cartwright et al., 2020). Consequently, robust drought monitoring frameworks are essential for estimating the intensity, duration, spatial extent, and recurrence patterns of droughts.

Various of drought indices have been developed to quantify meteorological and hydrological deficits. The Standardized Precipitation Index (SPI) (McKee et al., 1993) is widely used for precipitation-based drought assessments, whereas the Palmer Drought Severity Index (PDSI) (Palmer, 1965) incorporates soil moisture accounting. More recently, the Standardized Precipitation Evapotranspiration Index (SPEI) has gained prominence because it integrates both precipitation supply and atmospheric evaporative demand through a climatic water balance framework (Vicente-Serrano et al., 2010). By incorporating temperature-driven evapotranspiration, the SPEI is particularly suited for assessing drought under conditions of climate warming (Vicente-Serrano et al., 2012).

* Corresponding author. Institute of Geomatics and Civil Engineering, Faculty of Forestry, University of Sopron, Sopron, Hungary Bajcsy-Zs 4, Sopron, 9400, Hungary.
E-mail address: ix3mzk@uni-sopron.hu (A. Ahmed).

https://doi.org/10.1016/j.jaridenv.2026.105708
Received 12 February 2026; Received in revised form 22 July 2026; Accepted 23 July 2026
Available online 28 July 2026
0140-1963/

Several comparative studies suggest that SPEI may better capture climate change–induced drought intensification than the SPI, particularly in regions experiencing rising temperatures (Gumus, 2023; Li et al., 2020). Consequently, the SPEI has been widely applied in global and regional drought monitoring (Abu Arra and Şişman, 2024; Fuentes et al., 2022; Mokhtar et al., 2021; Salimi et al., 2021). Drought variability has been a defining climatic feature of the past century across the African Sahel. The prolonged Sahelian drought of the late 1960s through the 1980s caused widespread famine, ecological degradation, and population displacement (Nicholson et al., 2013). Although rainfall partially recovered after the 1990s, considerable debate persists regarding the extent, spatial heterogeneity, and sustainability of this recovery (Lebel and Ali, 2009; Nicholson et al., 2018). Recent analyses indicate increased rainfall variability and intensification of extreme events, rather than a simple return to pre-drought stability (Biasutti, 2019; Calim Costa et al., 2024).

Sudan represents a critical case within the Sahelian climate system because of its pronounced north south rainfall gradient and exposure to rapid climate variability (Alriah et al., 2024; Trummer et al., 2023). Historically, Sudan has experienced severe drought episodes in 1913, 1940, 1954, and most notably during 1980-1984, when widespread crop failure and famine affected millions (Atiem et al., 2022; Teklu et al., 1991). Rainfall declines between the 1960s and the 1980s were accompanied by increasing interannual variability, particularly in western Sudan, where the coefficients of variation rose substantially (Atiem et al., 2022; Siddig et al., 2022). Recent satellite-based studies have further demonstrated the value of integrating meteorological and remotely sensed data for drought monitoring across Sudan (Adam et al., 2026), while climate projections indicate increasing temperatures and changes in precipitation patterns that may alter future drought characteristics (Mohamed et al., 2024).

Darfur, located in western Sudan, is especially vulnerable to droughts because of its predominantly rain-fed agricultural systems and pastoral livelihoods. The region supports approximately 7.5 million people from diverse ethnic communities (Nagmeldin and Hanna, 2023; Nweke, 2021). Competition over land and water resources, exacerbated by environmental degradation, desertification, and weak governance, has contributed to recurrent conflict and displacement (Attaalmannan, 2019; Schimmer, 2007). Climate variability interacts with socio-political fragility, intensifying the vulnerability of internally displaced populations and agro-pastoral communities.

Despite the central role of drought in shaping environmental change and human livelihoods in Darfur, long-term assessments of drought dynamics are limited. Previous studies in Sudan have primarily focused on precipitation-based drought indices, agricultural impacts, and localized analyses (Elagib and Elhag, 2011; Elhag and Zhang, 2018; Mohmmed et al., 2018b). More recent satellite-based assessments have improved drought monitoring at the national scale (Adam et al., 2026), yet the long-term temporal evolution and regime dynamics of drought in Darfur have received comparatively little attention. In particular, few studies have combined standardized drought indices with non-stationary time-series approaches to distinguish gradual climatic trends from episodic shifts in drought behaviour. Addressing this gap is important for understanding hydroclimatic variability in one of the most climate-sensitive and conflict-affected regions of the Sahel.

The novelty of this study lies in the integration of the SPEI with complementary trend and breakpoint detection techniques to evaluate both long-term drought evolution and temporal regime shifts across Darfur. Unlike conventional linear trend analyses, the combined application of piecewise regression and the Breaks For Additive Seasonal and Trend (BFAST) method enables the identification of gradual climatic changes alongside episodic transitions in drought dynamics. We hypothesize that drought conditions in Darfur have undergone significant multi-decadal changes consistent with the broader hydroclimatic recovery reported for the Sahel, while exhibiting marked spatial heterogeneity among North, West, and South Darfur. Accordingly, the objectives of this study were to (1) quantify long-term drought variability across North, West, and South Darfur using theSPEI, (2) detect temporal breakpoints and regime shifts in drought evolution using piecewise regression and BFAST analyses, (3) compare drought dynamics among the three regions and relate them to broader hydroclimatic variability across Sudan and the Sahel, and (4) discuss the implications of long-term drought variability for drought monitoring, environmental management, and climate adaptation in arid environments.

2. Methods

2.1. Study area

Darfur is in western Sudan (Fig. 1) between 9°00′-18°56′ N and 23°54′-27°02′ E, covering approximately 531,000 km^2 and bordering Chad, Libya, South Sudan, and the Central African Republic (Ahmed et al., 2025). The region lies within the Sahelian belt and exhibits pronounced north-south climatic and ecological gradients. The climate ranges from arid desert conditions in the north to semi-arid and savannah conditions in the south. Rainfall is highly seasonal, occurring between June and September, with marked interannual variability (Ahmed et al., 2025). The northern areas receive low and erratic precipitation, whereas the southern and western sectors experience higher rainfall. Temperatures are high throughout the year, often exceeding 40 °C during the dry season (Ahmed et al., 2024).

Topographically, Darfur is flat to gently undulating, interrupted by the Jebel Marra volcanic massif, which rises above 3000 m above sea level (Hegazy et al., 2018). This highland system acts as a climatic and ecological divide, enhancing orographic rainfall and supporting cooler and wetter microclimates than the surrounding lowlands. Soil varies from sandy and nutrient-poor desert soils in the north to more fertile clay and loamy soil in central and southern areas (Hegazy et al., 2021). Vegetation follows a climatic gradient, with sparse xerophytic shrubs in the north, transitioning to woodland and savannah vegetation in the south. Dominant woody species include *Vachellia tortilis, Vachellia seyal*, *Senegalia senegal*, *Balanites aegyptiaca*, *Ziziphus spina-christi*, and *Combretum glutinosum*, while the Jebel Marra highlands support localized montane vegetation with relatively high floristic diversity (Hegazy et al., 2018). The regional economy is largely based on rain-fed agriculture and pastoralism, making it highly sensitive to drought variability, rainfall fluctuations, and land degradation.

2.2. SPEI-12 computation, trend analysis, and breakpoint detection

2.2.1. Data preparation

Monthly climatic records for the North, West, and South Darfur meteorological stations were compiled from structured spreadsheet datasets containing the year, month, precipitation (P), and air temperature (T). To ensure temporal consistency, each observation was assigned to the first day of the corresponding month, thereby standardizing the dataset to regular monthly time steps. The records were chronologically ordered and subjected to quality control procedures, including verification of valid month entries (1-12), removal of duplicate timestamps, and screening for temporal discontinuities. These steps ensured the construction of a continuous monthly time series suitable for drought index computation and subsequent time-series analyses. All preprocessing and analytical procedures were conducted using R statistical software.

2.2.2. SPEI calculation and conceptualization

Drought conditions were quantified using the SPEI, which was originally developed to represent standardized anomalies in the climatic water balance (Vicente-Serrano et al., 2010). The SPEI integrates both precipitation supply and atmospheric evaporative demand, making it particularly suitable for assessing drought under conditions of climate

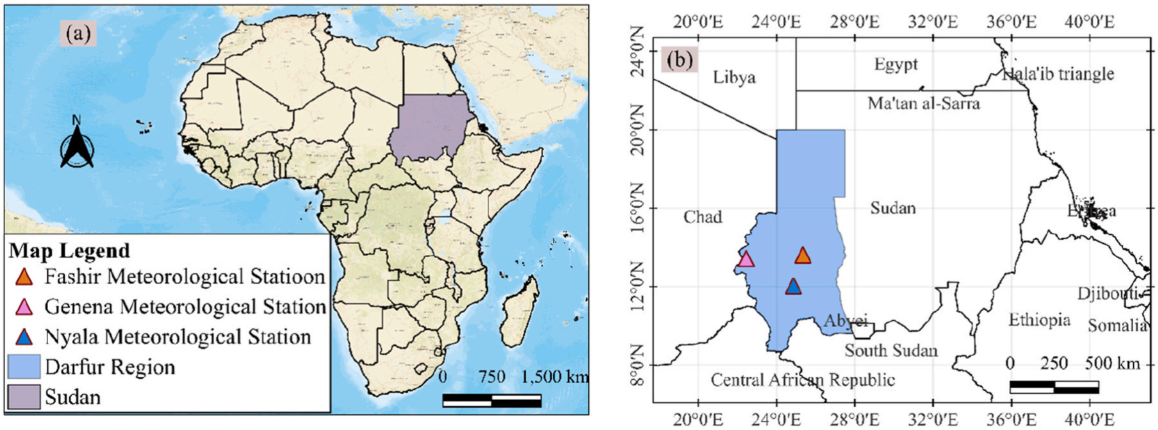

Fig. 1. Map of the study area shows (a) location of Sudan within Africa, and (b) location of Darfur region within Sudan.

variability and warming trends. Under a physically consistent formulation, SPEI is computed from the climatic water balance defined as precipitation minus potential evapotranspiration (P-PET). However, owing to the limited availability of PET data for the study area, the climatic water balance was approximated using Equation (1):

$$D_t = P_t \text{ - } Tt \quad (1)$$

Where D_t represents the monthly proxy water balance at time t_1 P_t is the monthly precipitation, and T_t is the monthly mean temperature. This formulation is explicitly treated as a proxy and interpreted cautiously, recognizing that temperature alone does not fully capture the evaporative demand. The methodological limitations are acknowledged in line with the recommendations from (Beguería and Vicente-Serrano, 2023). The monthly water-balance series were converted into regular time-series objects and standardized using the SPEI package in R, applying a 12-month aggregation window (SPEI-12). Aggregation was performed using a rolling accumulation procedure to capture cumulative moisture deficits over annual timescales. The leading and trailing missing values introduced by the accumulation window were removed to preserve statistical consistency. Although multiple accumulation scales were explored to capture different drought processes, SPEI-6 (short-to medium-term agricultural drought) and SPEI-12 (long-term hydrological and ecological drought), the present analysis emphasizes SPEI-12 because of its relevance to vegetation dynamics, water resources, and broader socio-environmental systems.

2.2.3. Drought classification

Drought events were classified according to the standardized thresholds proposed for SPEI (Abu Arra and Şişman, 2024; Vicente-Serrano et al., 2010). Based on these thresholds, drought frequency was defined as the number of occurrences in which SPEI values were ≤ -1.0, corresponding to at least moderate drought conditions in the study area. The drought classes used in this study were near-normal (SPEI ≥ -0.5), moderate drought ($-1.5 \leq$ SPEI < -1.0), severe drought ($-2.0 \leq$ SPEI < -1.5), and extreme drought (SPEI < -2.0). These thresholds are commonly used because they represent progressively increasing moisture deficits and facilitate comparison among regions and studies using standardized drought indices (Beguería et al., 2014). A drought event was considered to commence when SPEI decreased below -1.0 and to terminate when the index returned to a zero or positive value. Drought duration was calculated as the number of consecutive months with SPEI below -1.0, and drought severity was quantified as the cumulative SPEI deficit during each event (Bae et al., 2018; Serkendiz et al., 2024; Tirivarombo et al., 2018). Given the widespread application of these thresholds in recent drought studies across Sudan and other semi-arid regions, they provide a consistent basis for evaluating the temporal characteristics and intensity of climatic drought (Adam et al., 2026).

2.2.4. Trends analysis and breakpoint detection

(a) Structural Break Analysis

To detect non-stationarity and regime shifts in drought evolution, structural breakpoints were identified using the strucchange framework in R. A piecewise linear regression model was fitted, allowing for multiple slope changes over time, following Equation (2):

$$SPEI_t = \beta_0 + \beta_1 t + \varepsilon t \quad (2)$$

Candidate models with varying numbers of breakpoints were evaluated using the Bayesian Information Criterion (BIC), which balances the model fit against complexity (Zeileis et al., 2024). The model with the lowest BIC value was selected as the optimal model. To prevent the detection of spurious short-term fluctuations, a minimum segment length (expressed as a fraction of the total series length) was imposed. This penalized likelihood approach is widely applied in climate time-series analysis to objectively identify structural regime shifts.

(b) BFAST Decomposition

Complementary breakpoint detection was conducted using the Breaks For Additive Seasonal and Trend (BFAST) method (Verbesselt et al., 2010). BFAST decomposes a time series into seasonal, trendy, and residual components using Equation (3):

$$Y_t = S_t + T_t + e_t(t = 1, 2, 3, \ldots n) \quad (3)$$

Where:

Y_t is the observed SPEI-12 value at time t_i.

S_t represents the seasonal component.

T_t denotes the long-term trend component, potentially containing structural breaks.

e_t captures residual variability.

The iterative BFAST procedure identifies statistically significant changes in the trend and seasonal components, enabling the detection of abrupt drought regime shifts. In this study, BFAST was applied to the SPEI-12 series to detect long-term structural changes in drought dynamics in Darfur.

2.2.5. Piecewise trend estimation and uncertainty

Following breakpoint detection, ordinary least squares (OLS) linear regression models were fitted to each temporal segment to quantify the direction and magnitude of drought trends. Piecewise regression was selected because it provides a simple and interpretable estimate of the average rate of change within relatively homogeneous periods while allowing changes in trend between successive segments. Rather than assuming that the entire climatic record follows a single linear trajectory, this approach permits different linear relationships to be estimated where structural changes occur (Zeileis et al., 2003). For each segment, the slope (change in SPEI units yr^{-1}), coefficient of determination (R^2), and associated p-value were calculated. Predicted trend values together with their 95% confidence intervals were used to quantify the uncertainty associated with each fitted trend.

Because hydroclimatic time series often exhibit non-linear and non-stationary behaviour, piecewise regression was complemented with the BFAST method. Whereas piecewise regression quantifies long-term directional changes within each temporal segment, BFAST decomposes the time series into trend, seasonal, and remainder components and identifies abrupt temporal shifts that cannot be adequately represented by a single linear model (Verbesselt et al., 2010). The combined application of these approaches therefore enables both gradual long-term trends and episodic changes in drought dynamics to be characterized. Overall, the integration of SPEI-12, breakpoint detection, piecewise regression, and BFAST provides a robust framework for analysing drought variability in data-scarce dryland environments. All analyses were performed using R statistical software (R Core Team, 2020). and the complete analytical workflow is summarized in Fig. 2.

3. Results

3.1. Long-term piecewise trend in SPEI (1981-2025)

Piecewise linear regression identified a single long-term trend segment (1981–2025) for North, West, and South Darfur, with no structural break detected by the piecewise regression model during the study period (Table 1).

Positive slopes were observed in all three regions, although their magnitudes differed considerably (Table 1; Fig. 3). West Darfur recorded the highest rate of increase in SPEI-12 (0.0463 yr^{-1}), followed by South Darfur (0.0407 yr^{-1}), whereas North Darfur exhibited the lowest rate of increase (0.0198 yr^{-1}). The proportion of variance explained by the linear trend also varied spatially, with the highest coefficient of determination in West Darfur ($R^2 = 0.356$), followed by South Darfur ($R^2 = 0.277$) and North Darfur ($R^2 = 0.065$).

Table 1
Piecewise linear trend analysis of SPEI-12 (1981–2025).

Region	Slope (yr^{-1})	P-value	R^2
North Darfur	0.0198	<0.001	0.065
West Darfur	0.0463	<0.001	0.356
South Darfur	0.0407	<0.001	0.277

The temporal evolution of SPEI-12 differed among the three regions (Fig. 3). North Darfur (Fig. 3A) experienced severe drought episodes in 1983, 1984, 1991, 2004, and 2017, while moderate drought occurred in 1986, 1989, 1994, 1997, 2002, 2003, 2009, and 2011. West Darfur (Fig. 3B) experienced prolonged severe drought conditions between 1983 and 1991, interrupted by near-normal conditions in 1987, followed by another severe drought in 1998 and moderate drought in 1997, 2004, and 2011. South Darfur (Fig. 3C) recorded severe drought conditions during 1982–1987, interrupted by near-normal conditions in 1983 and 1985, with additional severe drought events in 1997 and 2017. Moderate drought persisted from 1988 to 1996 and reappeared in 2003 and 2010.

Across the three regions, drought conditions were concentrated during the 1980s and early 1990s, whereas the frequency of severe drought events decreased after the late 2000s. North Darfur recorded the largest number of isolated severe drought years during the later part of the study period, while West and South Darfur showed longer periods characterized by near-normal and wet conditions after approximately 2007.

3.2. Regional patterns of drought intensity at multiple timescales

Heatmaps of SPEI-6 and SPEI-12 illustrate temporal and regional differences in drought intensity across Darfur (Figs. 4 and 5). At the 6-month timescale (Fig. 4), North Darfur exhibited the highest frequency of moderate to severe drought conditions throughout the study period. South Darfur showed intermediate drought intensity, whereas West Darfur generally experienced fewer short-term drought events. Severe drought conditions occurred simultaneously across all three regions during the early 1980s, although their duration and intensity varied.

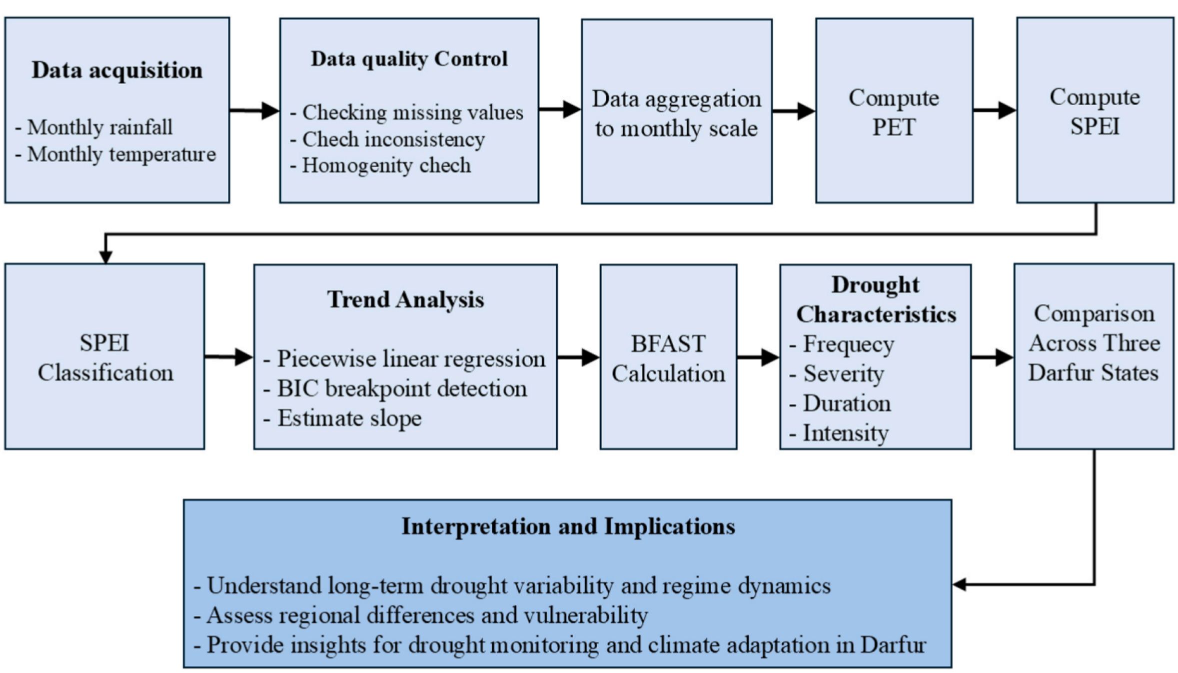

Fig. 2. Processing workflow.

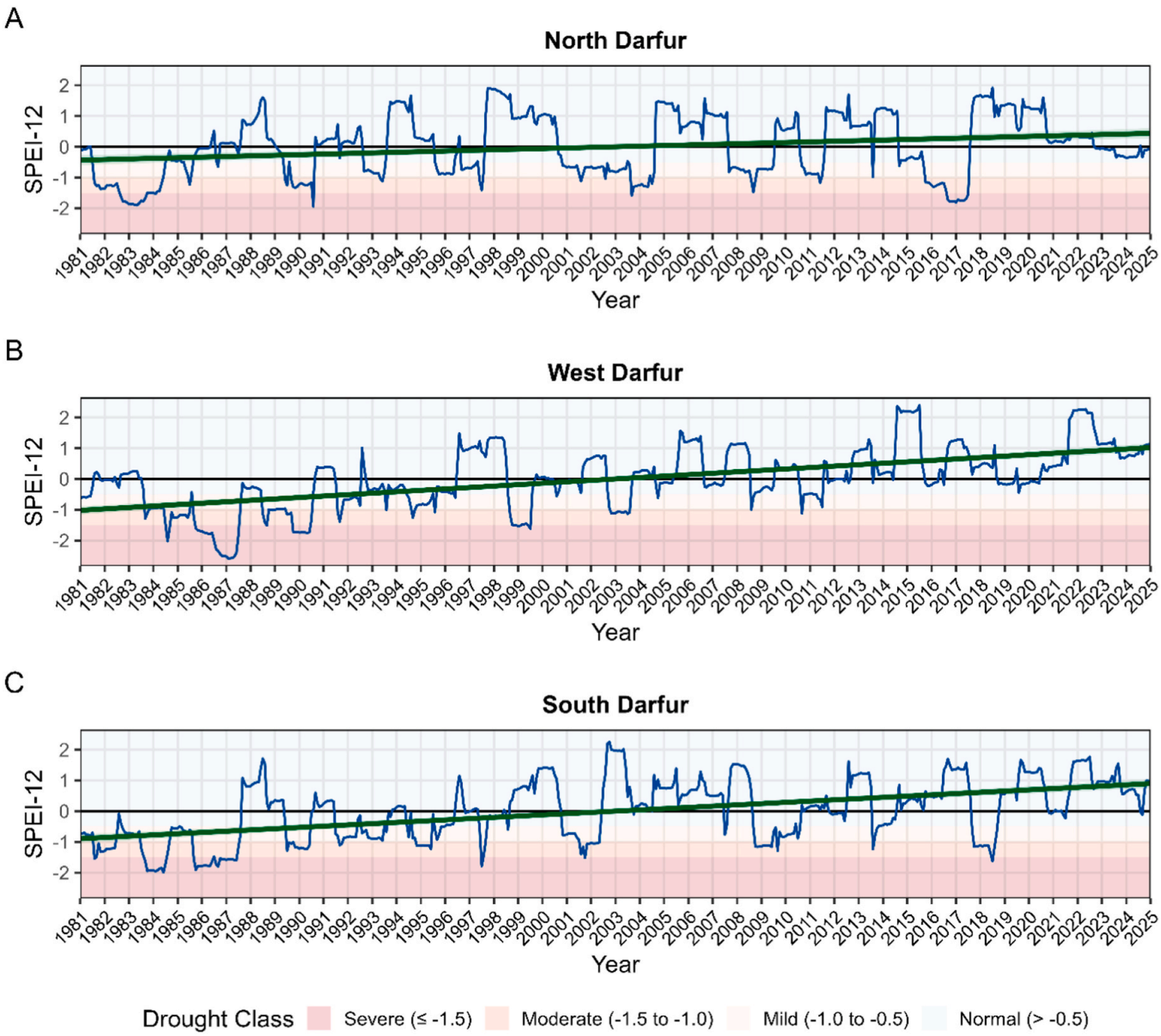

Fig. 3. SPEI-12 trends and drought classification for (A) North Darfur, (B) West Darfur, and (C) South Darfur during 1981–2025.

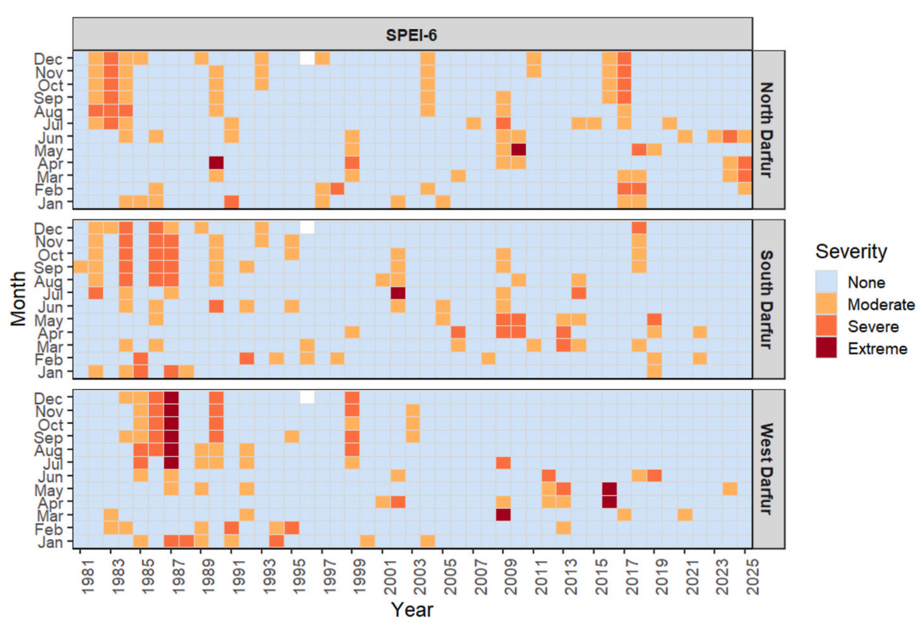

Fig. 4. Heatmap of SPEI-6 drought intensity across North, West, and South Darfur (1981–2025).

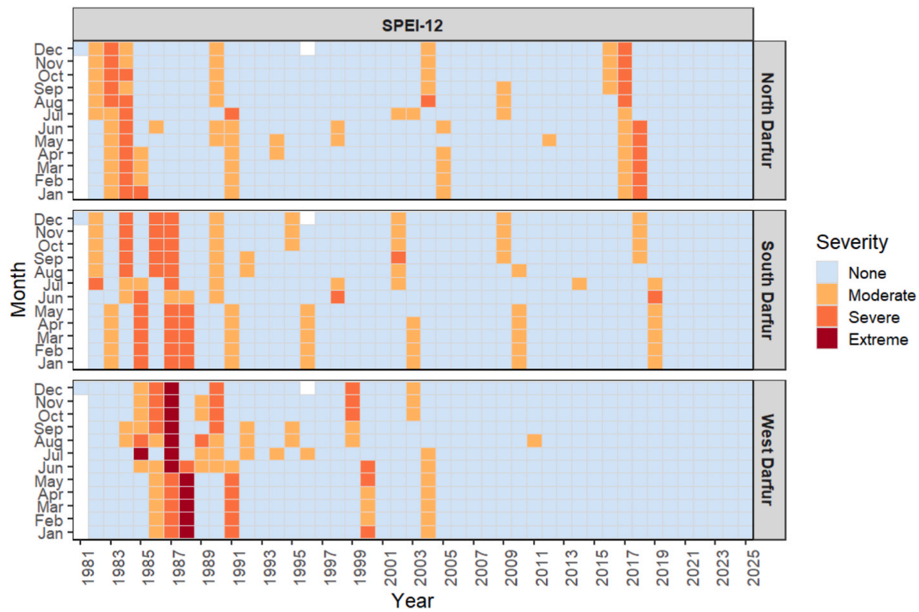

Fig. 5. Heatmap of SPEI-12 drought intensity across North, West, and South Darfur (1981–2025).

The 12-month SPEI (Fig. 5) showed similar regional differences but with greater persistence of drought episodes. West Darfur experienced extreme drought conditions between 1983 and 1988, while North and South Darfur were predominantly characterized by severe drought during the same period. From approximately 2007 onwards, West and South Darfur were dominated by near normal and positive SPEI values, whereas North Darfur continued to experience recurrent moderate and severe drought episodes.

3.3. Breakpoint detection using BFAST

BFAST analysis identified multiple breakpoints in the SPEI-12 time series across the three regions (Fig. 6). North Darfur exhibited five breakpoints (1990, 1998, 2005, 2014, and 2018), whereas West Darfur showed four breakpoints (1988, 1999, 2009, and 2018). South Darfur exhibited five breakpoints in 1988, 1995, 2007, 2009, and 2018. The timing of several breakpoints was common among the regions, particularly those occurring during the late 1980s and around 2018, although the intermediate breakpoints differed spatially. North Darfur displayed more frequent fluctuations throughout the study period, whereas West and South Darfur showed comparatively longer periods of uninterrupted trends between successive breakpoints. Following the breakpoints identified after the late 2000s, the SPEI-12 series in West and South Darfur was characterized by predominantly positive values, while North Darfur continued to exhibit alternating wet and dry conditions.

4. Discussion

4.1. Multi-decadal drought variability across Darfur

The SPEI-12 analysis revealed a significant positive trend across North, West, and South Darfur during 1981–2025, although the magnitude and persistence of the trend differed among the three

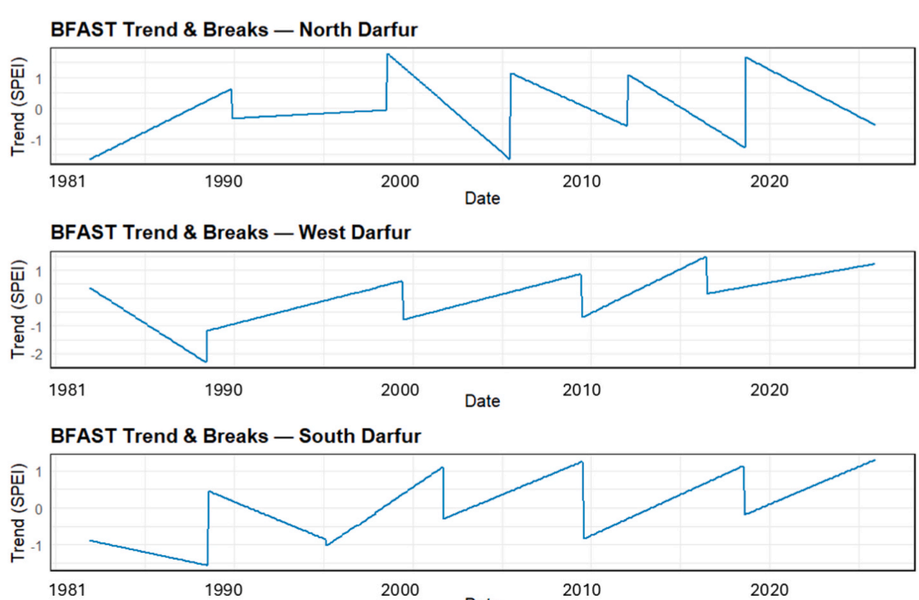

Fig. 6. BFAST decomposition of the SPEI-12 time series showing detected breakpoints for North, West, and South Darfur during 1981–2025.

regions. West Darfur exhibited the strongest increase in SPEI, followed by South Darfur, whereas North Darfur showed the weakest trend and the lowest proportion of the explained variance. These differences are consistent with the pronounced climatic gradient across Darfur, where annual rainfall increases from the hyper-arid northern plains toward the relatively wetter western and southern sectors influenced by the Jebel Marra highlands (Ahmed et al., 2025; Hegazy et al., 2021). Despite the positive long-term trend, severe drought events continued to occur throughout the study period, particularly in North Darfur. This persistence demonstrates that long-term changes in the climatic water balance do not necessarily translate into reduced drought occurrence at shorter temporal scales. Similar patterns have been reported for other dryland regions where gradual hydroclimatic recovery coexists with pronounced interannual variability (Abu Arra and Şişman, 2024). The comparatively low coefficient of determination observed in North Darfur further suggests that drought variability remains strongly controlled by year-to-year climatic fluctuations rather than long-term directional change. The BFAST analysis complements these findings by identifying several temporal breakpoints across the three regions, particularly during the late 1980s, late 1990s, and around 2018. These breakpoints likely represent shifts in climatic conditions superimposed on the long-term trend rather than persistent changes in the overall drought trajectory. Similar behaviour has been reported in non-stationary drought analyses where gradual climatic trends coexist with episodic hydroclimatic disturbances (Badawy et al., 2026; Granata and Di Nunno, 2025; Verbesselt et al., 2010).

4.2. Comparison with previous drought studies in Sudan

The observed multi-decadal evolution of drought conditions in Darfur agrees with previous studies conducted in Sudan, although important regional differences were evident (Elagib and Elhag, 2011). identified persistent drought conditions across large parts of Sudan associated with declining rainfall and increasing temperature during the second half of the twentieth century. Similarly (Mohmmed et al., 2018a), reported that North Darfur remains among the most drought-vulnerable regions because of recurrent rainfall deficits, land degradation, and limited adaptive capacity. The present study confirms the continued vulnerability of North Darfur while demonstrating that the region has also experienced a modest long-term increase in SPEI since the early 1980s.

Recent satellite-based drought assessments also support the spatial variability observed in this study. Using remotely sensed drought indicators (Elhag and Zhang, 2018), found considerable differences in drought severity across Sudanese agricultural regions, with western Sudan exhibiting substantial temporal variability. Likewise (Adam et al., 2026), demonstrated that satellite-derived drought indices capture regional differences in drought evolution across Sudan's rain-fed agricultural systems, reinforcing the importance of integrating climatic and spatial analyses for drought monitoring. Projected climate scenarios further suggest that rising temperatures and increasing rainfall variability will continue to influence drought conditions across Sudan (Mohamed et al., 2024). Consequently, the gradual increase in SPEI observed in the present study should not be interpreted as evidence of declining drought risk because increasing evaporative demand may offset future rainfall gains (Ahmed and Musa, 2020). The drought evolution observed in Darfur is consistent with the broader hydroclimatic recovery reported across Sahel (Biasutti, 2019; Nicholson, 2005; Sanogo, 2015).

4.3. Climate variability, environmental stress, and conflict dynamics

Darfur has been widely recognized as a region where climate variability interacts with socio-political vulnerabilities. Although climate change alone does not cause conflict, drought-related resource scarcity can exacerbate pre-existing tensions over land, water, and grazing corridors (IPCC, 2022; UNEP, 2024). The severe droughts of the 1980s contributed to large-scale environmental degradation, southward migration of pastoralists, and increased competition for fertile land, particularly along the Jebel Marra foothills. The clustering of extreme drought events in the early 1980s identified in this study coincides with the broader Sahel drought crisis that reshaped livelihood systems and settlement patterns across Sudan (Batterbury and Warren, 2001; Brooks, 2004). Subsequent partial moisture recovery since the 1990s may have moderated some ecological pressures, particularly in West and South Darfur. However, the persistence of episodic drought and high variability, especially in North Darfur, suggests that environmental stress remains structurally embedded in the region. Conflict climate linkages in arid environments operate through indirect pathways, drought reduces pasture productivity and crop yields, livelihood stress increases mobility and competition over limited water points, and weak governance and land tenure systems amplify disputes. Therefore, even under a long-term wetting trend, the recurrence of severe drought events can trigger localized stress in already fragile socio-ecological systems.

4.4. Policy implications for arid environment

The spatial differences observed among the three Darfur regions suggest that drought adaptation strategies should be geographically differentiated rather than being uniformly implemented. North Darfur is characterized by recurrent drought episodes and high interannual variability, indicating the need to prioritize water harvesting, rangeland restoration, and drought-resilient livelihood programs. Conversely, the comparatively stronger recovery observed in West and South Darfur provides opportunities for ecosystem restoration and sustainable agricultural intensification in these regions. These findings support recent recommendations advocating for integrated drought monitoring systems that combine climatic indices, satellite observations, and early warning information to strengthen resilience in crisis-affected drylands (Adam et al., 2026; Bogale et al., 2025; Mafi-Gholami and Jaafari, 2024).

4.5. Limitation and future research

This study has several limitations that should be considered when interpreting the results. First, the climatic water balance was approximated using a precipitation–temperature (P − T) proxy because potential evapotranspiration (PET) data were unavailable. Although this approach provides a useful indication of long-term drought variability, it may underestimate the influence of increasing atmospheric evaporative demand on drought severity under a warming climate.

Second, the analysis was based on station-derived meteorological observations, which provide robust temporal information but have limited spatial coverage. Consequently, the results characterize drought variability at the representative station locations rather than providing continuous spatial estimates across the entire Darfur region. Generating spatial drought probability maps or interpolated drought surfaces would require a denser observation network or the integration of gridded climate and remote sensing datasets, which was beyond the scope of the present study.

Future research should therefore integrate PET-based drought indices with satellite-derived products, including vegetation indices (e.g., NDVI), soil moisture, and land-use/land-cover datasets, to enable spatially explicit drought mapping and improve assessment of ecosystem responses to climate variability. The incorporation of gridded climate products and geostatistical or machine-learning approaches would further facilitate the development of drought probability maps and regional drought risk assessments. In addition, combining climatic indicators with remotely sensed observations and socio-economic datasets would improve understanding of the interactions among drought, vegetation dynamics, land degradation, livelihoods, and conflict in climate-sensitive drylands such as Darfur.

5. Conclusion

This study evaluated multi-decadal climatic drought variability in Darfur, Sudan, using SPEI-12, piecewise trend analysis and BFAST breakpoint detection. The results showed a long-term increase in SPEI across North, West, and South Darfur, indicating a gradual reduction in cumulative drought severity since 1981. However, the magnitude of change differed among regions, with West and South Darfur exhibiting stronger recovery than North Darfur, where drought variability remained relatively high.

Although the long-term trend was positive, severe drought episodes continued to occur throughout the study period, demonstrating that gradual hydroclimatic recovery has not eliminated the occurrence of extreme drought events. Breakpoint analysis further showed that drought evolution was characterized by episodic temporal shifts superimposed on an overall long-term trend.

These findings are consistent with the broader hydroclimatic recovery reported across the Sahel while emphasizing the considerable spatial variability that exists within Darfur. The results suggest that drought adaptation strategies should be tailored to regional conditions, with particular attention to North Darfur, where recurrent drought and high climatic variability continue to pose substantial environmental and livelihood challenges.

The integrated application of SPEI and non-stationary trend analysis provides a useful framework for monitoring drought dynamics in arid and semi-arid environments and can support climate adaptation, drought early warning, and sustainable natural resource management in Sudan and other drought-prone regions worldwide.

Funding

This research received funds from “the project TKP2021-NVA-13, which was implemented with the support provided by the Ministry of Culture and Innovation of Hungary from the National Research, Development and Innovation Fund, financed under the TKP2021-NVA funding scheme.”

CRediT authorship contribution statement

Abdalrahman Ahmed: Conceptualization, Data curation, Formal analysis, Methodology, Software, Validation, Writing – original draft, Writing – review & editing. **Kornel Czimber:** Funding acquisition, Supervision, Validation, Writing – original draft, Writing – review & editing.

Declaration of competing interest

The authors declare that they have no known competing financial interests or personal relationships that could have appeared to influence the work reported in this paper.

Acknowledgements

Our gratitude goes to the anonymous reviewers who helped improve the quality of the manuscript.

Data availability

Data will be made available on request.

References

Abu Arra, A., Şişman, E., 2024. A comprehensive analysis and comparison of SPI and SPEI for spatiotemporal drought evaluation. Environ. Monitor. Assessment 2024 196 (10), 980. https://doi.org/10.1007/S10661-024-13127-7, 196:10.

Adam, A.A., Musa, F.I., Lalruatkimi, C., Yasin, E.H.E., Thawmmawii, L., Alfadol, A.I.A., Khanna, N., Paul, A., Tripathi, O.P., Abdelmagid, T.D., Sahoo, U.K., Abushambo, A.A.K., Elyas, A.N.E., 2026. Satellite-based drought assessment in major Sudan's mechanized rain-fed agriculture. Sci. Rep. 2026 16 (1), 18650. https://doi.org/10.1038/s41598-026-49618-5, 16(1).

Ahmed, A., Rotich, B., Czimber, K., 2024. Assessment of the environmental impacts of conflict-driven Internally Displaced persons: a sentinel-2 satellite based analysis of land use/cover changes in the Kas locality, Darfur, Sudan. PLoS One 19 (5 May). https://doi.org/10.1371/journal.pone.0304034.

Ahmed, A., Rotich, B., Czimber, K., 2025. Climate change as a double-edged sword: exploring the potential of environmental recovery to foster stability in Darfur, Sudan. Climate 13 (3), 63. https://doi.org/10.3390/CLI13030063, 2025, Vol. 13, Page 63.

Ahmed, A., Rotich, B., Kipkulei, H.K., Lameck, A.S., Gallai, B., Czimber, K., 2025. Vegetation dynamics and climate variability in conflict zones: a case study of sortony internally displaced camp, Darfur, Sudan. Land 14 (8), 1680. https://doi.org/10.3390/LAND14081680, 2025, Vol. 14, Page 1680.

Ahmed, Shamseddin, Musa, 2020. Impacts of drought, food security policy and climate change on performance of irrigation schemes in Sub-Saharan Africa: the case of Sudan. Agric. Water Manag. 232, 106064. https://doi.org/10.1016/J.AGWAT.2020.106064.

Alahacoon, N., Edirisinghe, M., 2022. A comprehensive assessment of remote sensing and traditional based drought monitoring indices at global and regional scale. Geomat. Nat. Hazards Risk 13 (1), 762–799. https://doi.org/10.1080/19475705.2022.2044394.

Alriah, M.A.A., Bi, S., Nkunzimana, A., Elameen, A.M., Sarfo, I., Ayugi, B., 2024. Assessment of observed changes in drought characteristics and recent vegetation dynamics over arid and semiarid areas in Sudan. Theor. Appl. Climatol. 155 (5), 3541–3561. https://doi.org/10.1007/S00704-023-04824-3/FIGURES/11.

Asfaw, S., Pallante, G., Palma, A., 2021. Pathways for climate change adaptations in arid and semi-arid regions. J. Clean. Prod. 284, 124744. https://doi.org/10.1016/j.worlddev.2017.09.004.

Atiem, I.A., Siddig, M.S.A., Hamukwaya, S.L., Ahmed, H.I., Taha, M.M.M., Ibrahim, S., Osman, Y., 2022. Assessment of seasonal rainfall drought indices, Nyala City Sudan. Agriculture 2022 12 (7), 1069. https://doi.org/10.3390/agriculture12071069. Vol. 12, *Page 1069*.

Attaalmannan, 2019. Traditional tribal conflicts in Darfur reasons and seasons. J. Educ. Pract. https://doi.org/10.7176/JEP/10-32-11.

Badawy, H., Albanai, J., Hassan, A., 2026. Accelerating meteorological and ecological drought in arid coastal–mountain system: a 72-Year spatio-temporal analysis of Mount Elba Reserve using standardized precipitation evapotranspiration index. Land 15 (1). https://doi.org/10.3390/LAND15010202, 2026, Vol. 15.

Bae, S., Lee, S., Yoo, S., Water, T.K.-, 2018, undefined, 2018. Analysis of drought intensity and trends using the modified SPEI in South Korea from 1981 to 2010. Mdpi.Com. https://doi.org/10.3390/w10030327.

Batterbury, S., Warren, A., 2001. The African Sahel 25 years after the great drought: assessing progress and moving towards new agendas and approaches. Glob. Environ. Change 11 (1), 1–8. https://doi.org/10.1016/S0959-3780(00)00040-6.

Beguería, S., Vicente-Serrano, S.M., Reig, F., Latorre, B., 2014. Standardized precipitation evapotranspiration index (SPEI) revisited: parameter fitting, evapotranspiration models, tools, datasets and drought monitoring. Int. J. Climatol. 34 (10), 3001–3023. https://doi.org/10.1002/JOC.3887;ISSUE:ISSUE.

Beguería, S., Vicente-Serrano, S.M., 2023. Calculation of the Standardized Precipitation-Evapotranspiration Index [R Package SPEI Version 1.8.1]. CRAN: Contributed Packages. https://doi.org/10.32614/CRAN.

Biasutti, M., 2019. Rainfall trends in the African Sahel: characteristics, processes, and causes. Wiley Interdiscip. Rev. Clim. Change 10 (4), e591. https://doi.org/10.1002/wcc.591.

Bogale, T., Degefa, S., Dalle, G., Abebe, G., 2025. Spatio-temporal variations of drought in the Welmel watershed, southeast of Ethiopia using the vegetation condition index and standardized precipitation index. Ecol. Process. 14 (1), 37. https://doi.org/10.1186/S13717-025-00605-0, 2025 14:1.

Brooks, Nick, 2004. Drought in the African Sahel: long term perspectives and future prospects. Academia.Edu. https://www.academia.edu/download/78301254/tynwp61.pdf.

Calim Costa, M., Marengo, J.A., Alves, L.M., Cunha, A.P., 2024. Multiscale analysis of drought, heatwaves, and compound events in the Brazilian Pantanal in 2019–2021. Theor. Appl. Climatol. 155 (1), 661–677. https://doi.org/10.1007/S00704-023-04655-2/TABLES/6.

Cartwright, J.M., Dwire, K.A., Freed, Z., Hammer, S.J., McLaughlin, B., Misztal, L.W., Schenk, E.R., Spence, J.R., Springer, A.E., Stevens, L.E., 2020. Oases of the future? Springs as potential hydrologic refugia in drying climates. Front. Ecol. Environ. 18 (5), 245–253. https://doi.org/10.1002/fee.2191.

Dai, A., 2011. Characteristics and trends in various forms of the Palmer Drought Severity Index during 1900-2008. J. Geophys. Res. Atmos. 116 (12), 12115. https://doi.org/10.1029/2010JD015541.

Elagib, N.A., Elhag, M.M., 2011. Major climate indicators of ongoing drought in Sudan. J. Hydrol. 409 (3–4), 612–625. https://doi.org/10.1016/j.jhydrol.2011.08.047.

Elhag, K.M., Zhang, W., 2018. Monitoring and assessment of drought focused on its impact on sorghum yield over Sudan by using meteorological drought indices for the period 2001–2011. Remote Sens. 10 (8). https://doi.org/10.3390/RS10081231, 2018, Vol. 10.

Fuentes, I., Padarian, J., Vervoort, R.W., 2022. Spatial and temporal global patterns of drought propagation. Front. Environ. Sci. 10, 788248. https://doi.org/10.3389/fenvs.2022.788248.

Granata, F., Di Nunno, F., 2025. Evolving drought dynamics in Barcelona: leveraging a Bayesian ensemble algorithm for insightful analysis and a bidirectional long short-

term memory network for predictive modeling. Stoch. Environ. Res. Risk Assess. 39 (4), 1253–1270. https://doi.org/10.1007/S00477-024-02900-2, 2025 39:4.
Gumus, V., 2023. Evaluating the effect of the SPI and SPEI methods on drought monitoring over Turkey. J. Hydrol. 626 (1), 130386. https://doi.org/10.1016/j.jhydrol.2023.130386.
Hegazy, A.K., Hosni, H.A., El-Sheikh, M.A.R., Abo-El-Kassem, A., Badawi, E.S.M., Lovett-Doust, L., 2021. Plant biodiversity and soils in the Jebel Marra region of Darfur, Sudan. Arid Land Res. Manag. 35 (2), 127–161. https://doi.org/10.1080/15324982.2020.1819913.
Hegazy, A.K., Hosni, H.A., Kabiel, H.F., Badawi, E.S.M., Emam, M.H., Lovett-Doust, L., 2018. Population ecology of some keystone tree species in the Jebel Marra region of Darfur. Rendiconti Lincei 29 (3), 659–673. https://doi.org/10.1007/s12210-018-0701-z.
Hegazy, A.K., Kabiel, H.F., Hosni, H.A., Badawi, E.S.M., Lovett-Doust, L., 2018. Spatial and temporal variation in plant community phenology in the Jebel Marra region of Darfur. Folia Geobot. 53 (4), 389–403. https://doi.org/10.1007/s12224-018-9333-4.
IPCC, 2022. Climate change 2022: impacts, adaptation and vulnerability | climate change 2022: impacts, adaptation and vulnerability. https://www.ipcc.ch/report/ar6/wg2/.
Keshavarz, M., Karami, E., 2018. Drought and Agricultural Ecosystem Services in Developing Countries, pp. 309–359. https://doi.org/10.1007/978-3-319-90309-5_9.
Lebel, T., Ali, A., 2009. Recent trends in the central and Western Sahel rainfall regime (1990–2007). J. Hydrol. 375 (1–2), 52–64. https://doi.org/10.1016/j.jhydrol.2008.11.030.
Li, L., She, D., Zheng, H., Lin, P., Yang, Z.-L., Li, L., She, D., Zheng, H., Lin, P., Yang, Z.-L., 2020. Elucidating diverse drought characteristics from two meteorological drought indices (SPI and SPEI) in China. J. Hydrometeorol. 21 (7), 1513–1530. https://doi.org/10.1175/jhm-d-19-0290.1.
Liu, Y., Zhu, Y., Ren, L., Singh, V.P., Yuan, S., 2023. Flash drought fades away under the effect of accumulated water deficits: the persistence and transition to conventional drought. Environ. Res. Lett. 18 (11), 114035. https://doi.org/10.1088/1748-9326/ACFCCB.
Mafi-Gholami, D., Jaafari, A., 2024. Drought mapping, modeling, and remote sensing. Rem. Sens. Soil Land Surface Process.: Monitor. Mapp. Model. 303–313. https://doi.org/10.1016/B978-0-443-15341-9.00005-8.
McKee, T.B., Doesken, N.J., Kleist, J., 1993. The relationship of drought frequency and duration to time scales. Proceedi. 8th Confer. Appl. Clim. 17 (22), 179–183.
Mishra, A.K., Singh, V.P., 2010. A review of drought concepts. J. Hydrol. 391 (1–2), 202–216.
Mohamed, A.A.A., Maharana, P., Phartyal, S.S., Dimri, A.P., 2024. Projected change in precipitation and temperature over undivided Sudan and its major cities. Meteorol. Atmos. Phys. 136 (2), 11. https://doi.org/10.1007/S00703-024-01017-Z, 2024 136:2.
Mohmmed, A., Zhang, K., Kabenge, M., Keesstra, S., Cerdà, A., Reuben, M., Elbashier, M. M.A., Dalson, T., Ali, A.A.S., 2018a. Analysis of drought and vulnerability in the North Darfur region of Sudan. Land Degrad. Dev. 29 (12), 4424–4438. https://doi.org/10.1002/LDR.3180.
Mohmmed, A., Zhang, K., Kabenge, M., Keesstra, S., Cerdà, A., Reuben, M., Elbashier, M. M.A., Dalson, T., Ali, A.A.S., 2018b. Analysis of drought and vulnerability in the North Darfur region of Sudan. Land Degrad. Dev. 29 (12), 4424–4438. https://doi.org/10.1002/LDR.3180.
Mokhtar, A., Jalali, M., He, H., Al-Ansari, N., Elbeltagi, A., Alsafadi, K., Abdo, H.G., Sammen, S.S., Gyasi-Agyei, Y., Rodrigo-Comino, J., 2021. Estimation of SPEI meteorological drought using machine learning algorithms. IEEE Access 9, 65503–65523. https://doi.org/10.1109/ACCESS.2021.3074305.
Nagmeldin, K.-G., Hanna, R.-A., 2023. Ethnic diversity and its impact on group identification in Darfur. Ceeol.ComN Karamalla-Gaiballa, H Rubinkowska-AniołStudies in African Languages and Cultures, 2023•ceeol.Com 57. https://doi.org/10.32690/SALC57.1, 2023.
Nicholson, 2005. On the question of the "recovery" of the rains in the West African Sahel. J. Arid Environ. 63 (3), 615–641. https://doi.org/10.1016/j.jaridenv.2005.03.004.
Nicholson, Sharon, E., Acs, F., Bordi, I., Wang, D., 2013. The West African Sahel: a Review of Recent Studies on the Rainfall Regime and its Interannual Variability. Wiley Online Library, pp. 1–32. https://doi.org/10.1155/2013/453521, 2013.
Nicholson, S.E., Funk, C., Fink, A.H., 2018. Rainfall over the African continent from the 19th through the 21st century. Global Planet. Change 165, 114–127. https://doi.org/10.1016/J.GLOPLACHA.2017.12.014.
Nweke, A.C., 2021. Transition from Fragility to Sustainable Development: Case Study of Darfur in Sudan, 34. Walden University.
Palmer, D.S., 1965. Sequencing jobs through a multi-stage process in the minimum total time—A quick method of obtaining a near optimum. J. Oper. Res. Soc. 16 (1), 101–107. https://doi.org/10.1057/jors.1965.8.
R Core Team, 2020. R: the R project for statistical computing. https://www.r-project.org/.
Salimi, H., Asadi, E., Darbandi, S., 2021. Meteorological and hydrological drought monitoring using several drought indices. Appl. Water Sci. 11 (2), 11. https://doi.org/10.1007/s13201-020-01345-6, 2021 11:2.
Sanogo, S., 2015. Empirical analysis of the recent rainfall recovery in West Africa. http://197.159.135.214/jspui/handle/123456789/162.
Schimmer, R., 2007. Tracking the Genocide in Darfur: Population Displacement as Recorded by Remote Sensing. Yale Center for International and Area Studies, New Haven, CT, 36.
Serkendiz, H., Tatli, H., Kılıç, A., Çetin, M., Sungur, A., 2024. Analysis of drought intensity, frequency and trends using the SPEI in Turkey. Springer 155 (4), 2997–3012. https://doi.org/10.1007/s00704-023-04772-y.
Siddig, M.S.A., Ibrahim, S., Yu, Q., Abdalla, A., Osman, Y., Atiem, I.A., Hamukwaya, S.L., Taha, M.M.M., 2022. Bias adjustment of four satellite-based rainfall products using ground-based measurements over Sudan. Water 14 (9), 1475. https://doi.org/10.3390/w14091475, 2022, Vol. 14, Page 1475.
Sreeparvathy, V., Debdut, S., Mishra, A., 2025. A review of advances in flash drought research: challenges and future directions. Earths Future 13 (8), e2025EF006603. https://doi.org/10.1029/2025EF006603.
Teklu, T., Braun, J. Von, Zaki, E., 1991. Drought and famine relationships in Sudan: policy implications. https://books.google.com/books?hl=en&lr=&id=IEaXdkaoBeMC&oi=fnd&pg=PA11&ots=7MP9BALYeS&sig=XTTYb4K7fU19m68u_Ah3k3KPp6o.
Tirivarombo, S.O.D.E., Osupile, D., Eliasson, P., 2018. Drought monitoring and analysis: standardised precipitation evapotranspiration index (SPEI) and standardised precipitation index (SPI). Phys. Chem. Earth, Parts A/B/C 106, 1–10.
Trummer, U., Ali, T., Mosca, D., Mukuruva, B., Mwenyango, H., Novak-Zezula, S., 2023. Climate change aggravating migration and health issues in the African context: the views and direct experiences of a community of interest in the field. J. Migration Health 7, 100151. https://doi.org/10.1016/J.JMH.2023.100151.
UNEP, 2024. Sudan post-conflict environmental assessment | UNEP - UN environment programme. https://www.unep.org/sudan/sudan-post-conflict-environmental-assessment.
Verbesselt, J., Hyndman, R., Zeileis, A., Culvenor, D., 2010. Phenological change detection while accounting for abrupt and gradual trends in satellite image time series. Rem. Sens. Environ. 114 (12), 2970–2980. https://doi.org/10.1016/J.RSE.2010.08.003.
Vicente-Serrano, Sergio, Beguería, Santiago, López-Moreno, J.I., Vicente-Serrano, S.M., Beguería, S., López-Moreno, J.I., 2010. A multiscalar drought index sensitive to global warming: the standardized precipitation evapotranspiration index. J. Clim. 23 (7), 1696–1718. https://doi.org/10.1175/2009JCLI2909.1.
Vicente-Serrano, S.M., Beguería, S., López-Moreno, J.I., 2010. A multiscalar drought index sensitive to global warming: the standardized precipitation evapotranspiration index. J. Clim. 23 (7), 1696–1718. https://doi.org/10.1175/2009JCLI2909.1.
Vicente-Serrano, S.M., Beguería, S., Lorenzo-Lacruz, J., Camarero, J.J., López-Moreno, J. I., Azorin-Molina, C., et al., 2012. Performance of drought indices for ecological, agricultural, and hydrological applications. Earth Interact. 16 (10), 1–27. https://doi.org/10.1175/2012EI000434.1.
Zeileis, A., Kleiber, C., Walter, K., Hornik, K., 2003. Testing and dating of structural changes in practice. Comput. Stat. Data Anal. 44 (1–2), 109–123. https://doi.org/10.1016/S0167-9473(03)00030-6.
Zeileis, A., Leisch, F., Hornik, K., Kleiber, C., 2024. Testing, Monitoring, and Dating Structural Changes [R Package Strucchange Version 1.5-4]. CRAN: Contributed Packages. https://doi.org/10.32614/CRAN.